Science Advances
AAAS

advances.sciencemag.org/cgi/content/full/4/11/eaau4580/DC1

Supplementary Materials for

Autocrine-based selection of ligands for personalized CAR-T therapy of lymphoma

Alexey V. Stepanov, Oleg V. Markov, Ivan V. Chernikov, Daniil V. Gladkikh, Hongkai Zhang, Teresa Jones, Alexandra V. Sen'kova, Elena L. Chernolovskaya, Marina A. Zenkova, Roman S. Kalinin, Maria P. Rubtsova, Alexander N. Meleshko, Dmitry D. Genkin, Alexey A. Belogurov Jr., Jia Xie*, Alexander G. Gabibov*, Richard A. Lerner*

*Corresponding author. Email: jiaxie@scripps.edu (J.X.); gabibov@mx.ibch.ru (A.G.G.); rlerner@scripps.edu (R.A.L.)

Published 14 November 2018, *Sci. Adv.* **4**, eaau4580 (2018)
DOI: 10.1126/sciadv.aau4580

This PDF file includes:

Fig. S1. Structure of the reconstituted malignant BCR and combinatorial cyclopeptide library.
Fig. S2. Selected peptide ligands specifically interact with the malignant BCRs.
Fig. S3. Patient BCR-specific peptides on CAR activate reporter Jurkat cells transduced by membrane-tethered FL BCRs.
Fig. S4. FL–CAR-Ts do not eliminate Raji cells without exogenous lymphoma BCR.
Fig. S5. CTLs redirected by FL1-CAR infiltrate solid tumors and prevent xenograft metastasis.
Fig. S6. Malignant BCR recognizes self-antigen myoferlin.
Table S1. List of primers for amplification of variable region genes of heavy and light Ig chains.

SUPPORTING FIGURES

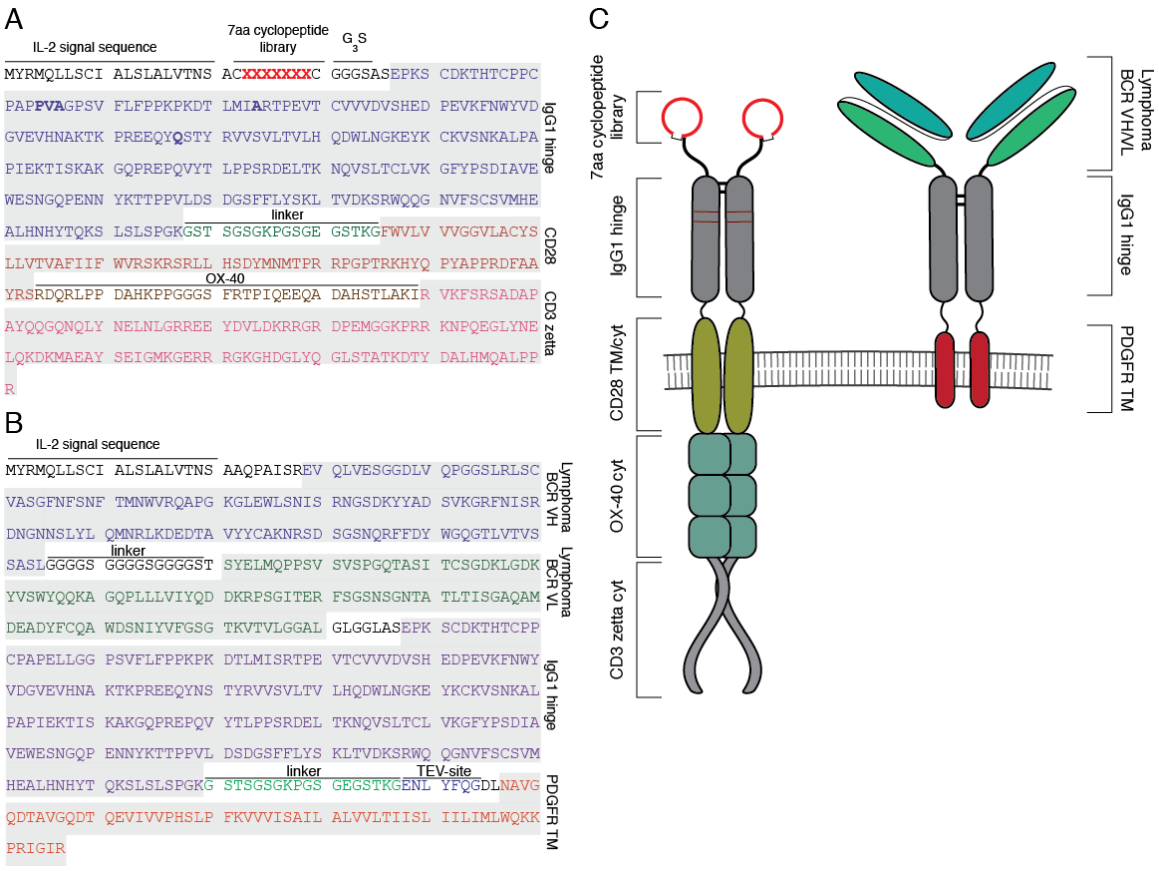

Fig. S1. Structure of the reconstituted malignant BCR and combinatorial cyclopeptide library. (**A**) Amino acid sequences of the combinatorial cyclopeptide library fused with chimeric antigen receptors signaling domains and (**B**) reconstituted malignant BCR fused with the IgG1 Fc hinge and membrane-spanning PDGFR domain. (**C**) Schematic representation of secreted molecules.

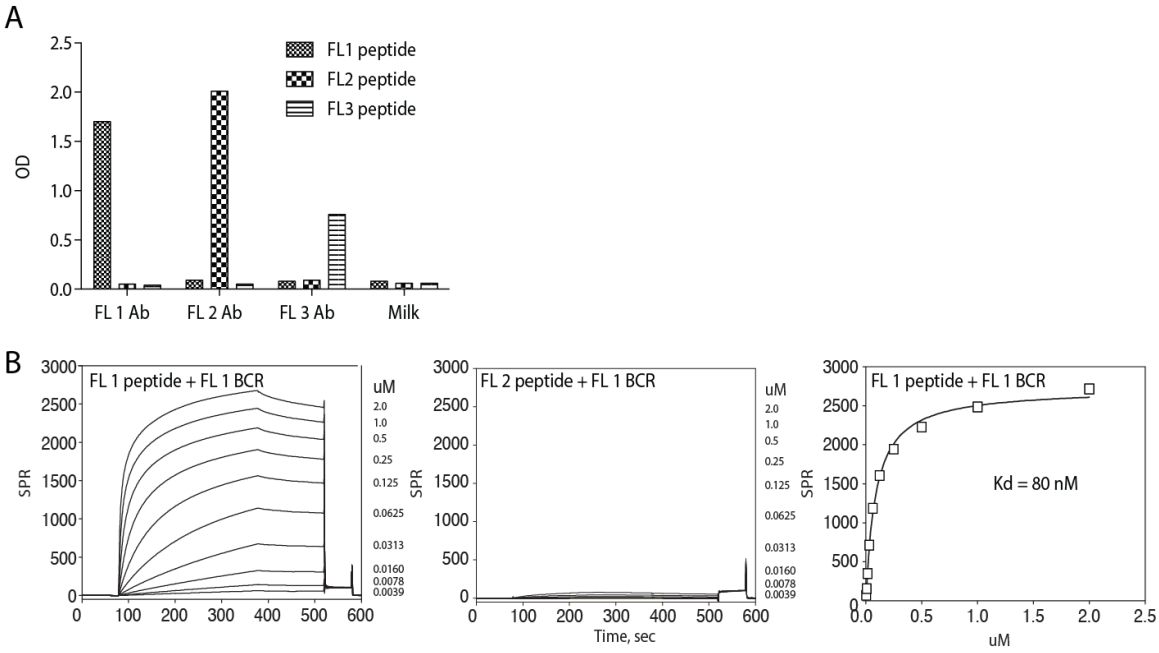

Fig. S2. Selected peptide ligands specifically interact with the malignant BCRs. (**A**) ELISA analysis of the interaction of the selected cyclopeptides FL1, FL2 and FL3 with the malignant BCRs. (**B**) SPR analysis of the interaction of the selected cyclopeptide FL1 and the malignant FL1 and FL2 BCR. Quantitative characteristics of FL1 Ab affinity to the identified FL1 peptide according to SPR data demonstrate strong interaction (Kd=80nM), while FL2 peptide does not have any affinity to the FL1 patient's BCR.

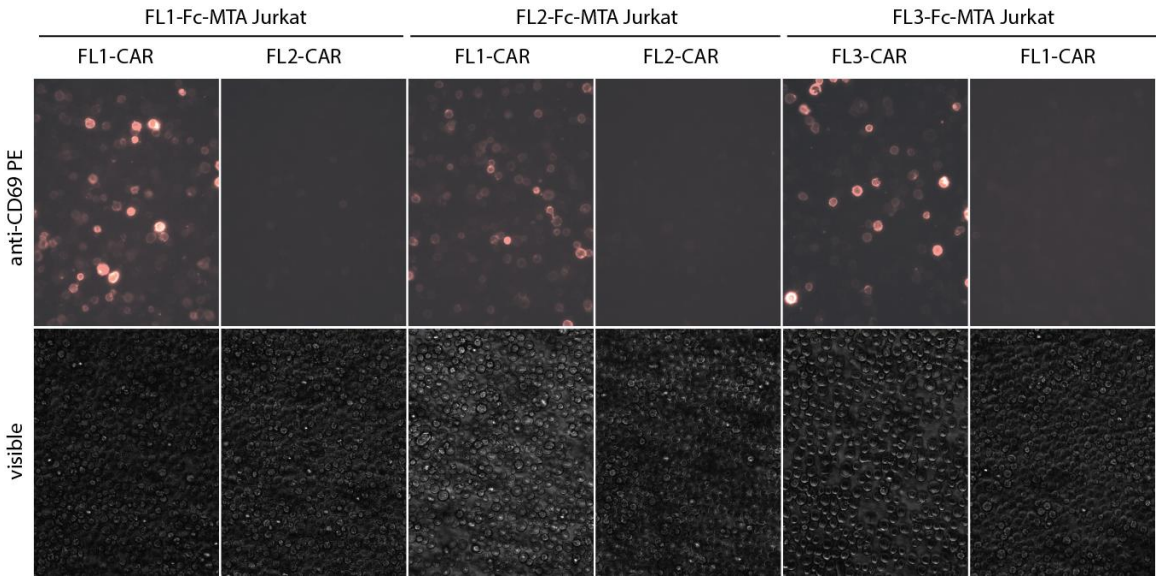

Fig. S3. Patient BCR-specific peptides on CAR activate reporter Jurkat cells transduced by membrane-tethered FL BCRs. Surface staining of reporter FL1-Fc-MTA, FL2-Fc-MTA and FL3-Fc-MTA Jurkat cells transduced with personalized CAR lentiviruses or lentiviruses with genes of another patient-specific CAR by antibody against CD69.

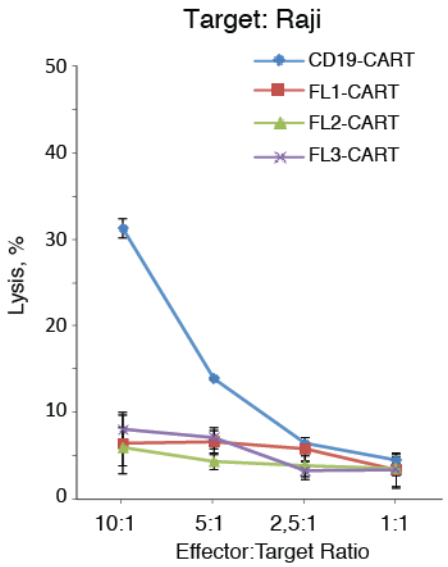

Fig. S4. FL–CAR-Ts do not eliminate Raji cells without exogenous lymphoma BCR. Only CD-19 CART showed killing activity on regular Raji cells. Minimum unspecific lysis was observed when FL1-CAR, FL2-CAR and FL3-CAR T cells were incubated with Raji cells. Cytotoxicity was determined by measuring lactate dehydrogenase release after 6 hours.

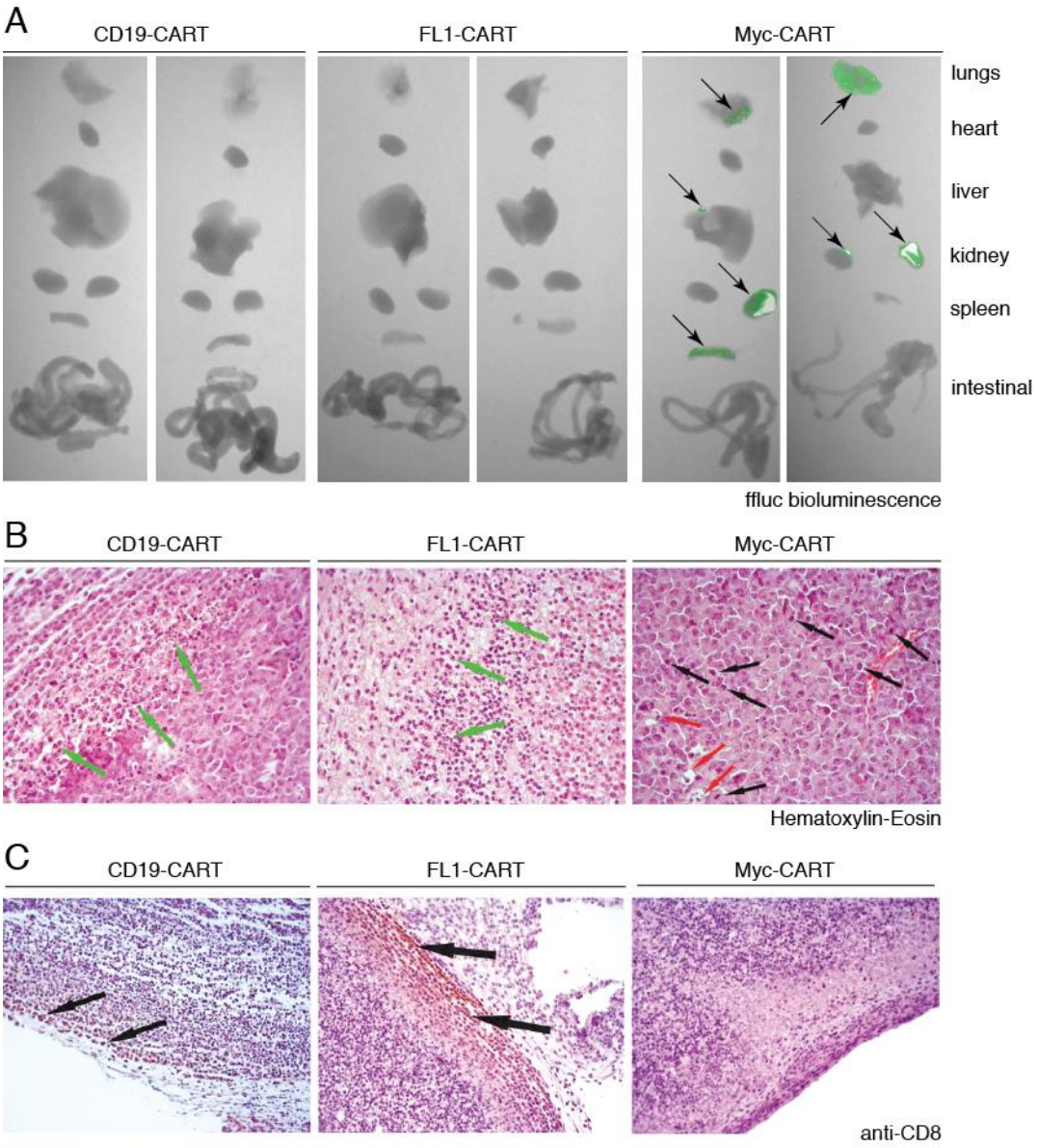

Fig. S5. CTLs redirected by FL1-CAR infiltrate solid tumors and prevent xenograft metastasis. (**A**) Bioluminescent imaging of organ-specific metastasis of Raji-FL1 cells (green) on day 35 after tumor implantation in mice treated by CD19-CART, FL1-CART and Myc-CART. For the Raji-FL1 cells detection mice received i.p. injection of the D-luciferine. (**B**) Histopathological changes analysis in tumors from CD19-CART, FL1-CART or Myc-CART treated animals. For identification of the histopathological changes tumors were stained with Hematoxylin-Eosin. Lymphoma B cells with basophilic cytoplasm and high mitotic rate indicated as black arrows. Macrophages containing cellular debris giving the characteristic “starry sky” appearance are indicated by red

arrows. Cells thought to be in the state of apoptosis are indicated by green arrows. (**C**) Immunohistochemical analysis of CD19-CART, FL1-CART or Myc-CART infiltration into the tumor (black arrows). The human CD8-specific antibodies were used for CART staining.

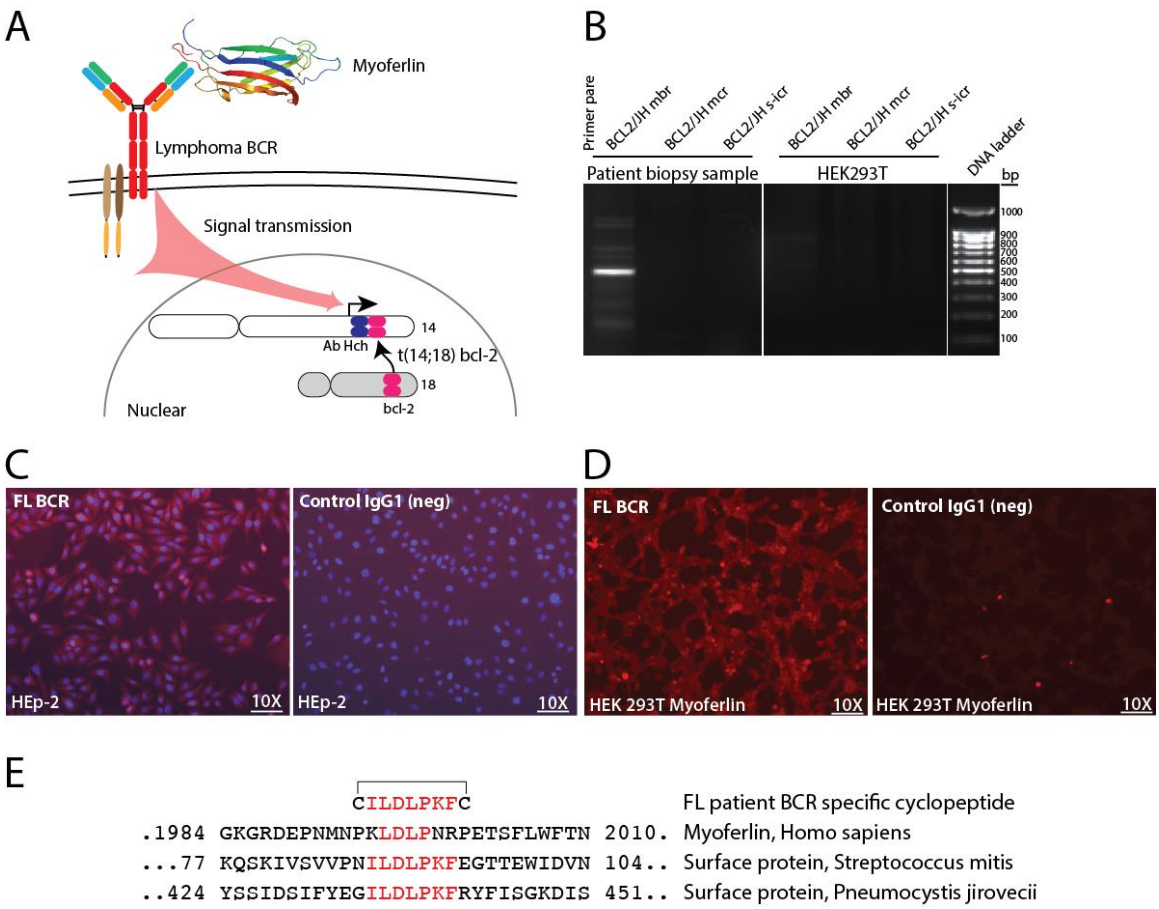

E

```
          CILDLPKFC                    FL patient BCR specific cyclopeptide
.1984 GKGRDEPNMNPKLDLPNRPETSFLWFTN 2010. Myoferlin, Homo sapiens
...77 KQSKIVSVVPNILDLPKFEGTTEWIDVN 104.. Surface protein, Streptococcus mitis
..424 YSSIDSIFYEGILDLPKFRYFISGKDIS 451.. Surface protein, Pneumocystis jirovecii
```

Fig. S6. Malignant BCR recognizes self-antigen myoferlin. (**A**) Schematically representation of myoferlin-driven autoreactive lymphomagenesis. (**B**) PCR analysis of bcl-2 rearrangement in FL patient 1 biopsy sample. Staining of HEp-2 cells (**C**) and myoferlin-expressing HEK293T cells (**D**) with soluble malignant BCR. (**E**) Alignment of the amino acid sequences of the identified malignant-specific peptide FL1 with the protein Myoferlin and surface proteins from *Streptococcus mitis* and *Pneumocytis jirovecii*.

Table S1. List of primers for amplification of variable region genes of heavy and light Ig chains.

Primer	Sequence 5'-3'	Orientation
L-VH1-start	ATGGACTGGACCTGGAGGATCCT	forward
L-VH2-start	ATGGACATACTTTGTTCCACGCTC	forward
L-VH3-start	ATGGAGTTTGGGCTGAGCTGG	forward
L-VH4-start	ATGAAACACCTGTGGTTCTTCCT	forward
L-VH5-start	ATGGGGTCAACCGCCATCCTC	forward
L-VH6-start	ATGTCTGTCTCCTTCCTCATCTTC	forward
IgM-3’	CTCTCAGGACTGATGGGAAGCC	reverse distal
IgM-clon	GGAGACGAGGGGGAAAAG	reverse proximal
IgG-3’	GCCTGAGTTCCACGACACC	reverse distal
IgG-clon	CAGGGGGAAGACCGATGG	reverse proximal
Vκ1-clon	GACATCCAGATGACCCAGTCTCC	forward
Vκ2-clon	GATATTGTGATGACCCAGACTCCA	forward
Vk3-clon	GAAATTGTGTTGACACAGTCTCCA	forward
IGKC-3’	CCCCTGTTGAAGCTCTTTGT	reverse distal
IGKC-clon	AGATGGCGGGAAGATGAAG	reverse proximal
VL1_(51)_clon	CAGTCTGTGTTGACGCAGCCGCCCTC	forward
VL1_(36-47)_clon	TCTGTGCTGACTCAGCCACCCTC	forward
VL1_(40)_clon	CAGTCTGTCGTGACGCAGCCGCCCTC	forward
VL2-clon	TCCGTGTCCGGGTCTCCTGGACAGTC	forward
VL3-clon	ACTCAGCCACCCTCGGTGTCAGTG	forward
VL4-clon	TCCTCTGCCTCTGCTTCCCTGGGA	forward
VL5-clon	CAGCCTGTGCTGACTCAGCC	forward
IGLC-3’	GTGTGGCCTTGTTGGCTTG	reverse distal
IGLC2-7_clon	CGAGGGGGCAGCCTTGGG	reverse proximal
IGLC1_clon	AGTGACCGTGGGGTTGGCCTTGGG	reverse proximal